Inorg. Chem. **2006**, *45*, 10629−10635

Inorganic Chemistry
Article

Polyoxometalate (W/Mo) Compounds Connected via Lanthanide Cations with a Three-Dimensional Framework, $H_2\{[K(H_2O)_2]_2[Ln(H_2O)_5]_2(H_2M_{12}O_{42})\}\cdot nH_2O$: Synthesis, Structures, and Magnetic Properties

Xiutang Zhang,[†,‡] Daqi Wang,[‡] Jianmin Dou,[‡] Shishen Yan,[§] Xinxin Yao,[§] and Jianzhuang Jiang*,[†]

Department of Chemistry, Shandong University, Jinan 250100, China, Department of Chemistry, Liaocheng University, Liaocheng 252000, China, and Department of Physics, Shandong University, Jinan 250100, China

Received July 7, 2006

A series of 10 novel polyoxometalate (W/Mo) compounds connected via a trivalent lanthanide cation bridge, $H_2\{[K(H_2O)_2]_2[Ln(H_2O)_5]_2(H_2M_{12}O_{42})\}\cdot nH_2O$ (Ln = La, Sm, Eu, Gd, Tb, Dy, Ho, Er, Yb, Lu; M = W or W/Mo) (**1**–**10**), were designed and synthesized on the basis of the abduction of Al^{3+} in aqueous solution. X-ray diffraction analyses reveal that the structures of complexes **1**–**10** are three-dimensional frameworks assembled from the arrangement of $H_2M_{12}O_{42}^{10-}$ (named paradodecmetalate-B) and $Ln(H_2O)_5^{3+}$ with two planes, which are constructed via the unification of $H_2M_{12}O_{42}^{10-}$ and $Ln(H_2O)_5^{3+}$, along the [100] and [001] directions. Magnetic measurements reveal the paramagnetic properties and a strong ferromagnetic coupling between the two nearest-neighboring lanthanide cations, Ln^{3+} (Ln = Dy, Er), within the circle for compounds **2** and **4**–**9**.

Introduction

The design of polyoxometalate clusters has attracted long-lasting research interest not only because of their appealing structural and topological novelty[1−4] but also because of their unusual optical, electronic, magnetic, and catalytic properties,[5−8] as well as their potential medical applications resulting from their antiviral properties and their inhibition of angiogenesis.[9] Most of the polyoxometalates reported thus far have been synthesized via the self-assembly of soluble precursors by means of the so-called reduction−oxidation−reconstitution technique in aqueous solution or under hydrothermal conditions.[10] Actually, the construction of polyoxometalates

---

[*] To whom correspondence should be addressed. E-mail: jzjiang@sdu.edu.cn.

[†] Shandong University.

[‡] Liaocheng University.

[§] Shandong University.

(1) (a) Pope, M. T.; Müller, A. *Angew. Chem., Int. Ed. Engl.* **1991**, *30*, 34−48. (b) Pope, M. T.; Müller, A. *Polyoxometalates: From Platonic Solids to Anti-Retroviral Activity;* Kluwer Academic Publishers: Dordrecht, The Netherlands 1994. (c) Pope, M. T. *Heteropoly and Isopoly Oxometalates;* Springer: New York, 1983.

(2) (a) Khan, M. I.; Müller, A.; Dillinger, S.; Bögge, H.; Chen, Q.; Zubieta, J. *Angew. Chem.* **1993**, *105*, 1811−1814. (b) Gaunt, A. J.; May, I.; Helliwell, M.; Richardson, S. *J. Am. Chem. Soc.* **2002**, *124*, 13350−13351. (c) Cronin, L.; Beugholt, C.; Krickemeyer, E.; Schmidtmann, M.; Bögge, H.; Kögerler, P.; Luong, T. K. K.; Müller, A. *Angew. Chem., Int. Ed.* **2002**, *41*, 2805−2808. (d) Wu, C. D.; Lu, C. Z.; Zhuan, H. H.; Huang, J. S. *J. Am. Chem. Soc.* **2002**, *124*, 3836−3837.

(3) (a) Howell, R. C.; Perez, F. G.; Jain, S.; Horrocks, W. D.; Rheingold, A. L., Jr.; Francesconi, L. C. *Angew. Chem., Int. Ed.* **2001**, *40*, 4031−4034. (b) Mialane, P.; Dolbecq, A.; Lisnard, L.; Mallard, A.; Marrot, J.; Sécheresse, F. *Angew. Chem., Int. Ed.* **2002**, *41*, 2398−2401. (c) Uchida, S.; Mizuno, N. *Chem.—Eur. J.* **2003**, *9*, 5850−5857. (d) Fukaya, K.; Yamase, T. *Angew. Chem., Int. Ed.* **2003**, *42*, 654−658. (e) Felices, L. S.; Vitoria, P.; Gutiúrrez-Zorrilla, J. M.; Reinoso, S.; Etxebarria, J.; Lezama, L. *Chem.—Eur. J.* **2004**, *10*, 5138−5146.

(4) (a) Long, D. L.; Abbas, H.; Kögerler, P.; Cronin, L. *Angew. Chem., Int. Ed.* **2005**, *44*, 3415−3419. (b) Errington, R. J.; Petkar, S. S.; Horrocks, B. R.; Houlton, A.; Lie, L. H.; Patole, S. N. *Angew. Chem., Int. Ed.* **2005**, *44*, 1254−1257. (c) Bassil, B. S.; Dickman, M. H.; Kortz, U. *Inorg. Chem.* **2006**, *45*, 2394−2396. (d) Boglio, C.; Lemière, G.; Hasenknopf, B.; Thorimbert, S.; Lacôte, E.; Malacria, M. *Angew. Chem., Int. Ed.* **2006**, *45*, 3324−3327.

(5) (a) Zhang, C.; Howell, R. C.; Luo, Q.-H.; Fieselmann, H. L.; Todaro, L. J.; Francesconi, L. C. *Inorg. Chem.* **2005**, *44*, 3569−3578. (b) Zhang, C.; Howell, R. C.; Scotland, K. B.; Perez, F. G.; Todaro, L.; Francesconi, L. C. *Inorg. Chem.* **2004**, *43*, 7691−7701. (c) Yamase, T. *Chem. Rev.* **1998**, *98*, 307−326. (d) Bösing, M.; Loose, I.; Pohlmann, H.; Krebs, B. *Chem.—Eur. J.* **1997**, *3*, 1232−1237. (e) Coronado, E.; Gómez-García, C. J. *Chem. Rev.* **1998**, *98*, 273−296.

(6) (a) Katsoulis, D. E. *Chem. Rev.* **1998**, *98*, 359−388. (b) Richardt, P. J. S.; Gable, R. W.; Bond, A. M.; Wedd, A. G. *Inorg. Chem.* **2001**, *40*, 703−709. (c) López, X.; Bo, C.; Poblet, J. M. *J. Am. Chem. Soc.* **2002**, *124*, 12574.

(7) (a) Kortz, U.; Mbomekalle, I. M.; Keita, B.; Nadjo, L.; Berthet, P. *Inorg. Chem.* **2002**, *41*, 6412−6416. (b) Rüther, T.; Hultgren, V. M.; Timko, B. P.; Bond, A. M.; Jackson, W. R.; Wedd, A. G. *J. Am. Chem. Soc.* **2003**, *125*, 10133−10143. (c) Ben-Daniel, R.; Neumann, R. *Angew. Chem., Int. Ed.* **2003**, *42*, 92−95.

10.1021/ic0612597 CCC: $33.50

Scheme 1. Related Reactions and Possible Reaction Mechanisms[a]

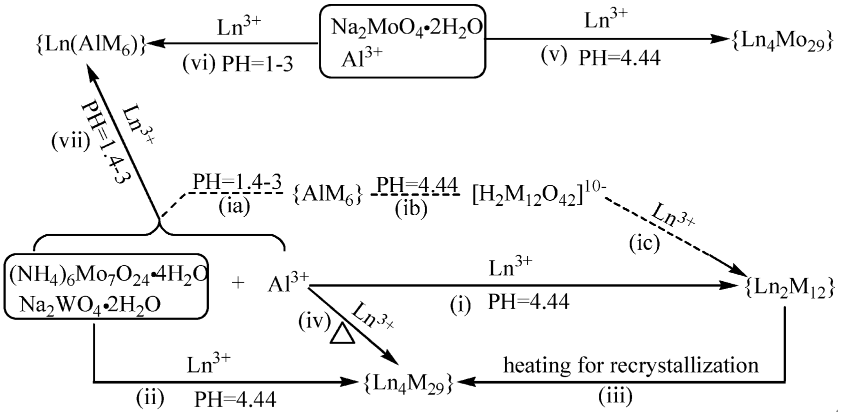

[a] Abbreviations: compounds **1**−**10**, $\{Ln_2M_{12}\}$; $[Ln_4(MO_4)H_2O)_{16}(M_7O_{24})_4]^{14-}$ anions, $\{Ln_4M_{29}\}$; $[Ln(H_2O)_7(AlM_6O_{24})]^{6-}$ anions, $\{Ln(AlM_6)\}$; $[Al(OH)_6M_6O_{18}]^{3-}$ anions, $\{AlM_6\}$.

obtained under these conditions is usually achieved by the connection of polyoxometalate building subunits via capping of the $\{MO_2\}$ groups using the two bridging oxygen atoms or secondary transition metals; in most cases, the transition metal ions exhibit the M−L (organic ligands) coordination mode or the metal−oxide framework.[11]

According to various coordination requirements and oxophilicity, lanthanide (Ln) cations have been introduced into polyoxometalates acting as an effective bridge to link discrete entities, such as Keggin (e.g., $SiW_{11}O_{39}^{8-}$), Anderson (e.g., $XMo_6O_{24}^{3-}$, X = Cr, Te), or $[Mo_{36}O_{108}(NO)_4(H_2O)_{16}]^{12-}$ units, to form new classes of large monoclusters, one- or two-dimensional polymolybdate materials with wide range of potential applications.[12−14] Recently, a few three-dimensional polyoxoanion-based architectures constructed from subunits of $[GdMo_{12}O_{42}]^{9-}$, $[Mo_{36}O_{108}(NO)_4(H_2O)_{16}]^{12-}$, $[Mo_6O_{19}]^{2-}$, $[IMo_6O_{24}]^{5-}$, and $[CrMo_6O_{24}]^{9-}$ connected via lanthanide bridges were also reported by Lu, Wang, Vladimir, and their co-workers.[15] Usually, these polyoxometalate complexes were provided by condensating trivalent lanthanide cations with the known polyoxometalate subunits.[12−15] However, it is still worth noting that the preparation of polyoxometalate (W/Mo) compounds with either known or novel subgroups using lanthanide cations as bridge is still a challenge because of the fast precipitation instead of crystallization of corresponding reaction product in the preparation process. Our research was therefore aimed toward the development of a new synthetic strategy to obtain polyoxometalate frameworks with lanthanide bridges.

In the present paper, we describe the synthesis of a series of novel polyoxo(mixed-metalate) (W/Mo) compounds connected via trivalent lanthanide cations, namely, $H_2\{K(H_2O)_2Ln(H_2O)_5[H_2M_{12}O_{42}]\}\cdot nH_2O$ (Ln = La, Sm, Eu, Gd, Tb, Dy, Ho, Er, Yb, Lu; M = W or W/Mo) (**1**−**10**), with a three-dimensional framework. Their single-crystal molecular structures, as well as the magnetic properties for compounds **2** and **4**−**9**, have also been systematically investigated.

Results and Discussion

Synthesis. As shown in Scheme 1, compounds $H_2\{K(H_2O)_2Ln(H_2O)_5[H_2M_{12}O_{42}]\}\cdot nH_2O$ (Ln = La, Sm, Eu, Gd, Tb, Dy, Ho, Er, Yb, Lu; M = W or W/Mo) (**1**−**10**) were successfully

---

(8) (a) Kim, W. B.; Voitl, T.; Rodriguez-Rivera, G. J.; Evans, S. T.; Dumesic, J. A. *Angew. Chem.* **2005**, *44*, 778−782. (b) Maayan, G.; Popovitz-Biro, R.; Neumann, R. *J. Am. Chem. Soc.* **2006**, *128*, 4968−4969. (c) Kumar, D.; Derat, E.; Khenkin, A. M.; Neumann, R.; Shaik, S. *J. Am. Chem. Soc.* **2005**, *127*, 17712−17718. (d) Kasai, J.; Nakagawa, Y.; Uchida, S.; Yamaguchi, K.; Mizuno, N. *Chem.*−*Eur. J.* **2006**, 4176−4184.

(9) (a) Judd, D. A.; Nettles, J. H.; Nevins, N.; Snyder, J. P.; Liotta, D. C.; Tang, J.; Ermolieff, J.; Schinazi, R. F.; Hill, C. L. *J. Am. Chem. Soc.* **2001**, *123*, 886−897. (b) Nomiya, K.; Torii, H.; Hasegawa, T.; Nemoto, Y.; Nomura, K.; Hashino, K.; Uchida, M.; Kato, Y.; Shimizu, K. *J. Inorg. Biochem.* **2001**, *86*, 657. (c) Aguey-Zinsou, K.-F.; Bernhardt, P. V.; Kappler, U.; McEwan, A. G. *J. Am. Chem. Soc.* **2003**, *125*, 530−535.

(10) (a) Khan, I. M.; Meyer, L. M.; Haushalter, R. C.; Schweitzer, A. L.; Zubieta, J.; Dye, J. L. *Chem. Mater.* **1996**, *8*, 43−53. (b) Khan, M. I.; Chen, Q.; Zubieta, J. *J. Chem. Soc., Chem. Commun.* **1993**, *4*, 356−357. (c) Gopalakrishnan, J. *Chem. Mater.* **1995**, *7*, 1265−1275. (d) Yamase, T.; Prokop, P. V. *Angew. Chem., Int. Ed.* **2002**, *41*, 466−469. (e) Müller, A.; Das, S. K.; Talismanov, S.; Roy, S.; Beckmann, E.; Bögge, H.; Schmidtmann, M.; Merca, A.; Berkle, A.; Allouche, L.; Zhou, Y. S.; Zhang, L. J. *Angew. Chem., Int. Ed.* **2003**, *42*, 5039−5044. (f) Müller, A.; Rehder, D.; Haupt, E. T. K.; Merca, A.; Bögge, H.; Schmidtmann, M.; Heinze-Brückner, G. *Angew. Chem., Int. Ed.* **2004**, *43*, 4466−4470.

(11) (a) Khan, M. I.; Chen, Q.; Salta, J.; O'Connor, C. J.; Zubieta, J. *Inorg. Chem.* **1996**, *35*, 1880−1901. (b) Reinoso, S.; Vitoria, P.; Lezama, L.; Luque, A.; Gutiérrez-Zorrilla, J. M. *Inorg. Chem.* **2003**, *42*, 3709−3711. (c) Burkholder, E.; Golub, V.; O'Connor, C. J.; Zubieta, J. *Inorg. Chem.* **2004**, *43*, 7014−7029. (d) Leclerc-Laronze, N.; Marrot, J.; Hervé, G. *Inorg. Chem.* **2005**, *44*, 1275−1281. (e) Xu, L.; Qin, C.; Wang, X. L.; Wei, Y. G.; Wang, E. B. *Inorg. Chem.* **2003**, *44*, 7342−7344.

(12) (a) Bartis, J.; Sukal, S.; Dankova, M.; Kraft, E.; Kronzon, R.; Blumenstein, M.; Francesconi, L. C. *J. Chem. Soc., Dalton Trans.* **1997**, 1937−1944. (b) Sadakane, M.; Dickman, M. H.; Pope, M. T. *Angew. Chem., Int. Ed.* **2000**, *39*, 2914−2916. (c) Mialane, P.; Lisnard, L.; Mallard, A.; Marrot, J.; Antic-Fidancev, E.; Aschehoug, P.; Vivien, D.; Sécheresse, F. *Inorg. Chem.* **2003**, *42*, 2102−2108.

(13) (a) Niu, J. Y.; Guo, D. J.; Wang, J. P.; Zhao, J. W. *Cryst. Growth Des.* **2004**, *4*, 241−247. (b) Lü, J.; Shen, E. H.; Li, Y, G.; Xiao, D. R.; Wang, E. B.; Xu, L. *Cryst. Growth Des.* **2005**, *5*, 65−67. (c) Ai, H. Y.; Wang, E. B.; Xiao, D. R.; Li, Y. G.; Xu, L. *Inorg. Chem. Commun.* **2005**, *8*, 267−270.

(14) (a) Wang, J. P.; Zhao, J. W.; Duan, X. Y.; Niu, J. Y. *Cryst. Growth Des.* **2006**, *6*, 507−513. (b) An, H. Y.; Li, Y. G.; Xiao, D. R.; Wang, E. B.; Sun, C. Y. *Cryst. Growth Des.* **2006**, *6*, 1107−1112.

(15) (a) Wang, X. L.; Guo, Y. Q.; Li, Y. G.; Wang, E. B.; Hu, C. W.; Hu, N. H. *Inorg. Chem.* **2003**, *42*, 4135−4140. (b) An, H. Y.; Lan, Y.; Li, Y. G.; Wang, E. B.; Hao, N.; Xiao, D. R.; Duan, L. Y.; Xu, L. *Inorg. Chem. Commun.* **2004**, *7*, 356−358. (c) An, H. Y.; Guo, Y. Q.; Li, Y. G.; Wang, E. B.; Lu, J.; Xu, L.; Hu, C. W. *Inorg. Chem. Commun.* **2004**, *7*, 521−523. (d) An, H. Y.; Xiao, D. R.; Wang, E. B.; Li, Y. G.; Wang, X. L.; Xu, L. *Eur. J. Inorg. Chem.* **2005**, 854−859.

isolated from the reaction of $Na_2WO_4 \cdot 2H_2O$ and $(NH_4)_6Mo_7O_{24} \cdot 4H_2O$ with related lanthanide cations, Ln^{3+}, in the presence of aluminum sulfate as abduction agent. It is worth noting that the role of aluminum sulfate as an abduction agent can be clearly demonstrated by the similar reaction of $Na_2WO_4 \cdot 2H_2O$ and $(NH_4)_6Mo_7O_{24} \cdot 4H_2O$ with the corresponding lanthanide cations in the absence of aluminum sulfate under the same reaction conditions, which led to the formation of $[Ln_4(MO_4)(H_2O)_{16}(M_7O_{24})_4]^{14-}$ anions, which areanalogous to reported ions.[17] Scheme 1 outlines the proposed formation reaction mechanism for compounds **1**−**10** with a three-dimensional framework. The Anderson anion, $[Al(OH)_6M_6O_{18}]^{3-}$, was formed from reaction ia with a pH value in the range of 1.4−3 and stirring. This is in agreement with the reported result of $[Ln(H_2O)_7(AlM_6O_{24})]^{6-}$ formed from reactions ovi and vii in the same pH range (1.4−3.0).[13c,16] In addition to the increase in the pH value, the reconstitution reaction occurs on the Anderson anion framework $[Al(OH)_6M_6O_{18}]^{3-}$, leading to the formation of an unstable intermediate, $H_2M_{12}O_{42}{}^{10-}$, via the loss of aluminum cations. The unstable intermediate, $H_2M_{12}O_{42}{}^{10-}$, then assembles with Ln^{3+} and K^+ to form the three-dimensional framework of $K(H_2O)_2Ln(H_2O)_5(H_2M_{12}O_{42})^{2-}$.

It is worth mentioning that during our exploration of the synthetic pathways, it has been found that substitution of potassium acetate by other alkali acetate salts, such as LiAc, NaAc, RbAc, CsAc, or NH_4Ac, added to adjust the pH value in reaction i, usually leads to the isolation of a powder product or few crystal salts consisting of $M_7O_{24}{}^{6-}$ instead of crystalline salts composed of paradodecmetalate-B ($H_2M_{12}O_{42}{}^{10-}$). This indicates that cations of K^+, Ln^{3+}, or both are the favorable basic construction units in the synthesis of polyoxometalate clusters with three-dimensional framework (vide infra).

Additionally, it is noteworthy that although crystalline compounds of $H_2\{K(H_2O)_2Ln(H_2O)_5[H_2M_{12}O_{42}]\} \cdot nH_2O$ (**1**−**10**) can be obtained from the aqueous solution of $Na_2WO_4 \cdot 2H_2O$, $(NH_4)_6Mo_7O_{24} \cdot 4H_2O$, and $Al_2(SO_4)_3 \cdot 18H_2O$ in the presence of lanthanide nitrate and potassium acetate, the experimental procedure must be controlled very carefully to avoid precipitation, which will lead to the isolation of powder product. In particular, heat must be avoided because of the very easy transformation from $\{K(H_2O)_2Ln(H_2O)_5[H_2M_{12}O_{42}]\}^{2-}$ to $[Ln_4(MO_4)(H_2O)_{16}(M_7O_{24})_4]^{14-}$. This is verified by the isolation of $[Ln_4(MO_4)(H_2O)_{16}(M_7O_{24})_4]^{14-}$ as a coproduct for most of the target compounds, $H_2\{K(H_2O)_2Ln(H_2O)_5[H_2M_{12}O_{42}]\} \cdot nH_2O$, including **1**, **2**, **3**, **4**, **5**, **9**, and **10**. Moreover, the change in the concentration of the starting materials resulted in the formation of powder product containing both $\{K(H_2O)_2Ln(H_2O)_5[H_2M_{12}O_{42}]\}^{2-}$ and $[Ln_4(MO_4)(H_2O)_{16}(M_7O_{24})_4]^{14-}$ instead of the pure target crystal compounds.

Structure Studies. All the compounds, **1**−**10**, crystallize in the same monoclinic crystal system with space group $P2_1/n$. Their unit cell contains one anion with the asymmetric unit consisting of one-quarter of the molecule. Crystallographic data and details of the diffraction experiments for compounds **1**−**10** are listed in Table 1. Elemental analyses show that tungsten occupies most of the M sites in the molecular structure, the ratio of W/Mo being 6.59−10.00 for compounds **1**−**10**. However, it must be pointed out that, because of the similar ionic radii of Mo^{6+} and W^{6+}, 0.59 and 0.60 Å,[18] some M sites are actually occupied by these two different metal atoms, but the sum of the occupancies of Mo/W was constrained to be 1 in the structural refinements.

As mentioned in the Introduction section, polymolybdate (W/Mo) complexes reported thus far connected via lanthanide cations, as a bridge, usually have one- or two-dimensional frameworks, and the three-dimensional examples are still relatively rare. However, single-crystal X-ray diffraction analyses for the newly prepared complexes **1**−**10** have revealed that they all have three-dimensional frameworks assembled from the arrangement of $H_2M_{12}O_{42}{}^{10-}$ and $Ln(H_2O)_5{}^{3+}$ with two planes in the [100] and [001] directions. The central anion of $H_2M_{12}O_{42}{}^{10-}$, analogous to paradodecatungstate B ($H_2W_{12}O_{42}{}^{10-}$),[19,20] consists of two types of corner-sharing groups of M_3O_{13} and M_3O_{14} with octahedron geometries of MO_6.

In compounds **1**−**10**, each polyanion of $H_2M_{12}O_{42}{}^{10-}$ acts as a 6-dentate ligand that links six Ln^{3+} cations, forming the remarkable three-dimensional frameworks, Figure 1, in a staggered manner. As shown in Figure 2, two neighboring $H_2M_{12}O_{42}{}^{10-}$ moieties are connected through two different types of linkage by cations of $Ln(H_2O)_5{}^{3+}$ in the [100] or [001] direction: (i) the first linkage involves two bridging $Ln(H_2O)_n{}^{3+}$ units connected via four terminal oxygen atoms from two symmetrical MO_2 units, forming the square circle (OW(1A)O−Ln(1A)−OW(1C)O−Ln(1B)), which is to some degree similar to the linkage in the reported dimeric anion of $[Eu(H_2O)_3(R\text{-}2\text{-}P_2W_{17}O_{61})]_2{}^{14-}$,[21] and (ii) the second linkage involves the two cations of $Ln(H_2O)_n{}^{3+}$ in the square circle coordinating to another two neighboring $H_2M_{12}O_{42}{}^{10-}$ moieties via the terminal oxygen atom of MO_2. Just like the two vertical planes of [100] and [001], the circles described above also adopt vertical directions. In turn, each cation of Ln^{3+}, acting as a joint, links three central anions of $H_2M_{12}O_{42}{}^{10-}$ via the terminal oxygen atoms of MO_2. The

---

(16) (a) Manikumari, S.; Shivaiah, V.; Das, S. K. *Inorg. Chem.* **2002**, *41*, 6953−6955. (b) Crystallographic data for $H_3[Al(OH)_6Mo_6O_{18}] \cdot 10H_2O$: $a = 11.3112$ Å, $b = 10.9279$ Å, $c = 11.7440$ Å, $\beta = 99.409°$.

(17) (a) Fedosseev, A. M.; Grigore, M. S.; Yanovskii, A. I.; Struchkovyn, T.; Spitsin, V. I. *Dokl. Akad. Nauk SSSR* **1987**, 111. (b) Naruke, H.; Ozeki, T.; Yamase, T. *Acta Crystallogr., Sect. C* **1991**, *47*, 489−492. (c) Cai, X. Z.; Wang, S. M.; Huang, J. F.; Guan, H. M.; Lin, X. *Chin. J. Struct. Chem.* **1997**, *16*, 328−334.

(18) (a) Shannon, R. D. *Acta Crystallogr., Sect. A* **1976**, *32*, 751−767. (b) Goubin, F.; Guénée, L.; Deniard, P.; Koo, H.-J.; Whangbo, M. H.; Montardi, Y.; Jobic, S. *J. Solid State Chem.* **2004**, *177*, 4528−4534.

(19) (a) Ina, L.; Michael, B.; Rita, K.; Bernt, K.; Rolf P. S.; Bernd, S. *Inorg. Chim. Acta* **1997**, *263*, 99. (b) Allmann, R. *Acta Crystallogr., Sect. B* **1971**, *27*, 1393−1404. (c) Evans, H. T., Jr.; Rollins, O. W. *Acta Crystallogr., Sect. B* **1976**, *32*, 1565−1567.

(20) Gimenez-Saiz, C.; Galan-Mascaros, J. R.; Triki, S.; Coronado, E.; Ouahab, L. *Inorg. Chem.* **1995**, *34*, 524−526. (e) Yan, B. B.; Goh, N. K.; Chia, L. S. *Inorg. Chim. Acta* **2004**, *357*, 490−494.

(21) Luo, Q. H.; Howell, R. C.; Bartis, J.; Dankova, M.; Horrocks, W. D., Jr.; Rheingold, A. L.; Francesconi, L. C. *Inorg. Chem.* **2002**, *41*, 6112−6117.

Table 1. Crystallographic Data and Details of Diffraction Experiments for Compounds **1**−**10**

	1	**2**	**3**	**4**
formula	$H_{88}K_4La_4W_{21.56}Mo_{2.44}O_{124}$	$H_{96}K_4Sm_4W_{22.04}Mo_{1.96}O_{128}$	$H_{96}K_4Eu_4W_{21.32}Mo_{2.68}O_{128}$	$H_{96}K_4Gd_4W_{21.56}Mo_{2.44}O_{128}$
mol mass (g/mol)	6982.64	7142.66	7085.81	7128.07
cryst syst	monoclinic	monoclinic	monoclinic	monoclinic
cryst size (mm)	0.14 × 0.08 × 0.08	0.16 × 0.08 × 0.06	0.08 × 0.06 × 0.04	0.12 × 0.06 × 0.04
space group	P2(1)/n	P2(1)/n	P2(1)/n	P2(1)/n
a (Å)	12.514(3)	12.552(7)	12.5196(17)	12.5228(19)
b (Å)	17.057(3)	17.099(10)	17.023(2)	17.024(3)
c (Å)	12.904(3)	13.103(7)	13.0213(17)	13.0389(19)
β (deg)	106.37(3)	106.440(8)	106.442(2)	106.330(2)
V (Å^3)	2642.7(9)	2697(3)	2661.6(6)	2667.7(7)
Z	1	1	1	1
d_{calcd} (g/cm^3)	4.388	4.397	4.421	4.437
μ (mm^{-1})	25.497	26.035	25.842	26.149
T (K)	298(2)	298(2)	298(2)	298(2)
measured reflns	13801	17374	13846	13847
unique reflns	4657	6516	4697	4707
R_{int}	0.0376	0.0532	0.0458	0.0331
refined params	364	362	382	363
2θ range (deg)	2.00 to 25.01	1.98 to 28.30	2.02 to 25.00	1.99 to 25.01
R [$I > 2\sigma(I)$]	R1= 0.0333[a]	R1 =0.0466[a]	R1 = 0.0425[a]	R1 = 0.0296[a]
	wR2 = 0.0888[b]	wR2 =0.1113[b]	wR2 = 0.1073[b]	wR2 = 0.0681[b]
R (all data)	R1 =0.0398[a]	R1 =0.0746[a]	R1 = 0.0425[a]	R1 = 0.0453[a]
	wR2 =0.0929[b]	wR2 =0.1277[b]	wR2 = 0.1073[b]	wR2 = 0.0751[b]
GOF[c]	1.001	1.002	1.002	1.001
$(\Delta\rho)_{max}$ (e$^-$/Å^3)	3.135	6.247	3.638	3.297
$(\Delta\rho)_{min}$ (e$^-$/Å^3)	−4.78	−5.528	−6.277	−1.997

	5	**6**	**7**
formula	$H_{96}K_4Tb_4W_{20.88}Mo_{3.12}O_{128}$	$H_{96}K_4Dy_4W_{20.96}Mo_{3.04}O_{128}$	$H_{84}K_4Ho_4W_{20.84}Mo_{3.16}O_{122}$
mol mass (g/mol)	7074.97	7096.32	6987.40
cryst syst	monoclinic	monoclinic	monoclinic
cryst size (mm)	0.16 × 0.08 × 0.06	0.12 × 0.11 × 0.10	0.12 × 0.11 × 0.10
space group	P2(1)/n	P2(1)/n	P2(1)/n
a (Å)	12.542(3)	12.5367(12)	12.5205(14)
b (Å)	17.052(3)	17.0436(17)	16.9983(19)
c (Å)	12.936(3)	12.8239(13)	12.8130(15)
β (deg)	106.37(3)	106.1910(10)	106.1940(10)
V (Å^3)	2654.4(9)	2631.4(5)	2618.8(5)
Z	1	1	1
d_{calcd} (g/cm^3)	4.426	4.478	4.431
μ (mm^{-1})	25.790	26.244	26.414
T (K)	298(2)	298(2)	298(2)
measured reflns	13525	20965	18448
unique reflns	4685	5455	4607
R_{int}	0.0532	0.0540	0.0715
refined params	363	364	354
2θ range (deg)	2.00 to 25.01	2.04 to 26.50	2.01 to 25.01
R [$I > 2\sigma(I)$]	R1 = 0.0413[a]	R1 = 0.0557[a]	R1 = 0.0487[a]
	wR2 = 0.1078[b]	wR2 = 0.1398[b]	wR2 = 0.1241[b]
R (all data)	R1 = 0.0556[a]	R1 = 0.0595[a]	R1 = 0.0538[a]
	wR2 = 0.1178[b]	wR2 = 0.1426[b]	wR2 = 0.1277[b]
GOF[c]	1.000	1.000	1.002
$(\Delta\rho)_{max}$ (e$^-$/Å^3)	4.680	4.874	5.107
$(\Delta\rho)_{min}$ (e$^-$/Å^3)	−5.024	−9.799	−6.117

	8	**9**	**10**
formula	$H_{96}K_4Er_4W_{21.16}Mo_{2.84}O_{128}$	$H_{84}K_4Yb_4W_{22}Mo_2O_{122}$	$H_{96}K_4Lu_4W_{21.76}Mo_{2.24}O_{128}$
mol mass (g/mol)	7132.94	7121.81	7216.53
cryst syst	monoclinic	monoclinic	monoclinic
cryst size (mm)	0.16 × 0.08 × 0.06	0.10 × 0.06 × 0.04	0.16 × 0.08 × 0.06
space group	P2(1)/n	P2(1)/n	P2(1)/n
a (Å)	12.503(3)	12.491(3)	12.531(6)
b (Å)	16.992(3)	16.989(3)	17.070(8)
c (Å)	12.813(3)	12.786(3)	13.066(6)
β (deg)	106.12(3)	106.06(3)	106.375(6)
V (Å^3)	2615.1(9)	2607.3(9)	2682(2)
Z	1	1	1
d_{calcd} (g/cm^3)	4.529	4.536	4.469
μ (mm^{-1})	26.955	28.221	27.413
T (K)	298(2)	298(2)	298(2)
measured reflns	18579	13640	13956
unique reflns	4599	4583	4722
R_{int}	0.0744	0.0383	0.0318

Table 1. Continued

	8	**9**	**10**
refined params	382	380	363
2θ range (deg)	2.01 to 25.01	2.02 to 25.01	2.02 to 25.01
R [$I > 2\sigma(I)$]	R1 = 0.0424[a]	R1 = 0.0373[a]	R1 = 0.0456[a]
	wR2 = 0.0984[b]	wR2 = 0.0965[b]	wR2 = 0.1274[b]
R (all data)	R1 = 0.0524[a]	R1 = 0.0514[a]	R1 = 0.0566[a]
	wR2 = 0.1030[b]	wR2 = 0.1058[b]	wR2 = 0.1358[b]
GOF[c]	1.003	1.002	1.002
$(\Delta\rho)_{max}$ (e$^-$/Å^3)	2.389	2.627	4.495,
$(\Delta\rho)_{min}$ (e$^-$/Å^3)	−2.949	−5.527	6.336

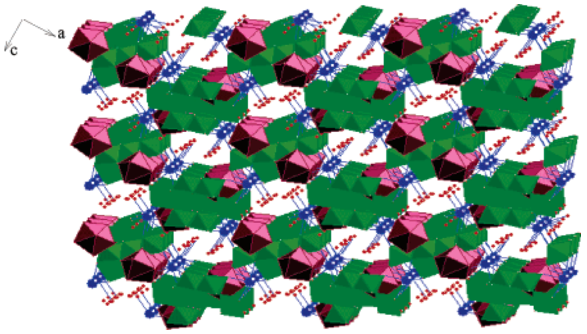

Figure 1. Packing diagram of compounds **1**−**10** viewed down the *c* axis. The octahedra represent MO_6 (green) and LnO_8 (dark red), and the balls are K^+ (blue) and O (red).

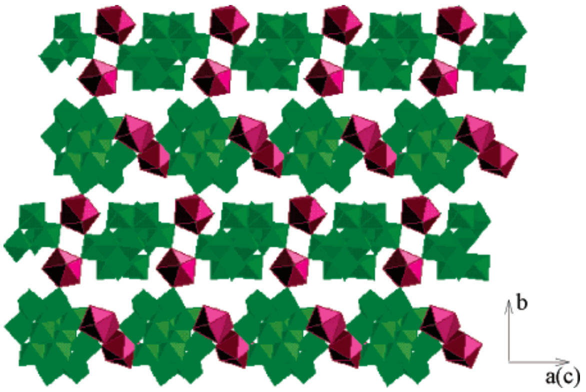

Figure 2. Connectivity pattern in the crystal structures of compounds **1**−**10**, constructed via the unification of $H_2M_{12}O_{42}^{10-}$ and $Ln(H_2O)_5^{3+}$ along the [100] and [001] directions. The octahedra represent MO_6 (green) and LnO_8 (dark red).

coordinated oxygen atoms around each Ln^{3+} can be divided into two classes according to different sources. The first one contains five aqua ligands with a Ln−O_{water} distance of 2.263−2.664 Å, Table 2. The other contains three terminal oxygen atoms of tungsten/molybdenum with a Ln−$O_{terminal}$ length in the range of 2.306−2.477 Å. As shown in Table 2, the observed decrease of the Ln−$O_{terminal}$ and Ln−O_{water} bond lengths in the series of Sm^{III}, Eu^{III}, Gd^{III}, Tb^{III}, Dy^{III}, Ho^{III}, Er^{III}, and Yb^{III}, along with the decrease in the lanthanide ionic size, suggests the effect of the lanthanide contraction.[22,6c]

Table 2. Comparison of Selected Bond Lengths (Å) of Ln−O_{water} and Ln−$O_{terminal}$ in Compounds **1**−**10**

	Ln−O_{water}	Ln−$O_{terminal}$
1	2.333−2.505	2.353−2.442
2	2.397−2.664	2.394−2.477
3	2.346−2.545	2.358−2.456
4	2.301−2.519	2.376−2.453
5	2.327−2.481	2.342−2.459
6	2.309−2.460	2.336−2.437
7	2.296−2.443	2.321−2.433
8	2.296−2.380	2.308−2.434
9	2.263−2.455	2.306−2.419
10	2.280−2.455	2.363−2.466

For compounds **1**−**10**, the extended network of hydrogen bonds involving water molecules and oxygen atoms of the central oxoanions exists in the staggered three-dimensional frameworks. The extended structure of **1**−**10** contains small voids, which are occupied by lattice water molecules. By neglecting all lattice water molecules, we show that the effective size of the pores is about 1368 Å^3 per unit cell,[23] ~52% of the crystal volume. The lattice water molecules in the voids are bonded to the terminal oxygen atoms of molybdenum and to the aqua ligands of the Ln^{III} cations through the relative weak hydrogen bonding with O···O distances of 2.99(2)−3.04(2) Å.

The assignment of the oxidation states for the tungsten/molybdenum is consistent with the electric charge and confirmed by bond valence sum calculations,[24] by which the range and average valence sum for the tungsten/molybdenum atoms are 5.84−5.96 and 5.90 for **1**, 5.86−5.94 and 5.90 for **2**, 5.86−5.95 and 5.90 for **3**, 5.83−5.96 and 5.90 for **4**, 5.82−5.99 and 5.90 for **5**, 5.86−5.96 and 5.90 for **6**, 5.86−5.96 and 5.90 for **7**, 5.86−5.98 and 5.92 for **8**, 5.85−6.02 and 5.91 for **9**, and 5.85−5.95 and 5.90 for **10**, respectively.

Magnetic Measurements. To reveal the nature of interactions between the rare earth cations in these lanthanide bridged-polyoxometalate complexes, magnetic measurements have been conducted on these newly prepared samples. Figures 3, 4, and S2−S13 (Supporting Information) show the magnetization curves, *M*−*H*, at 2 K and the temperature dependence of susceptibility, χ−*T*, at the magnetic field of 10 000 Oe for compounds **2** and **4**−**9**, respectively.

As shown in Figure 3, the *M*−*H* curve of compound **6** shows a typical paramagnetic feature. As a result, the *M*−*H* curve of this compound is fitted by the Langevin function, $M = N\mu_0(cth(\mu_0H/kT) - kT/\mu_0H)$, where *M* is the magnetization, *N* is the number of the ions (or magnetic clusters) per mole, and μ_0 is the moment per ions (or per magnetic cluster).[25] On the basis of the best fitting, the parameters $\mu_0 = 17.28\ \mu_B$ and $N = 8.23 \times 10^{23}$ are obtained, among which the value $N = 8.23 \times 10^{23}$ is smaller than the expected one

---

(22) Gautier, R.; Andersen, O. H.; Gougeon, P.; Halet, J.-F.; Canadell, E.; Martin, D. D. *Inorg. Chem.* **2002**, *41*, 4689−4699.

(23) van der Sluis, P.; Spek, A. L. PLATON program. *Acta Crystallogr., Sect. A* **1990**, *46*, 194−201.

(24) Brese, N. E.; O'Keeffe, M. *Acta Crystallogr., Sect. B* **1991**, *47*, 192−197.

(25) O'Handley, R. C. *Modern Magnetic Materials: Principles and Applications*; Wiley: New York, 2000; p 76.

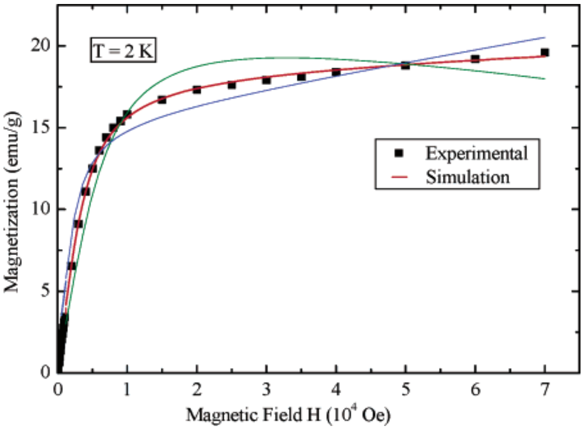

Figure 3. Dependence of magnetization on the external magnetic field for compound **6** at 2 K (red line, fitting to the experimental data; green line, simulation by one Dy^{3+} cation moment; blue line, simulation by the moment of three Dy^{3+} cations).

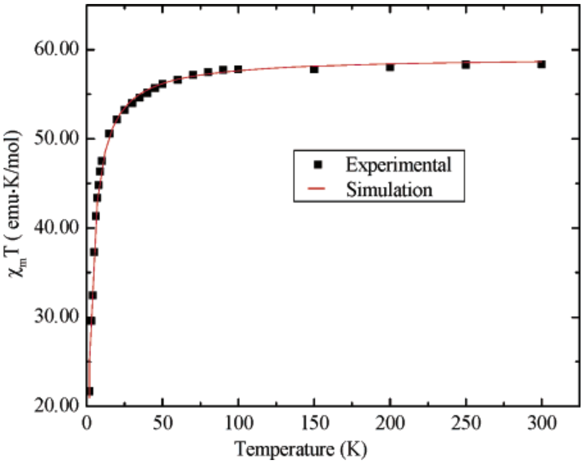

Figure 4. Molar magnetic susceptibility as a function of temperature for compound **6** measured at external magnetic field of 10 000 Oe.

($N = 24.08 \times 10^{23}$). It is clear that the magnetic moment value obtained for this compound, 17.28 μ_B, is larger than the magnetic moment of the single Dy^{3+} cation (10 μ_B) but smaller than the moments of two Dy^{3+} cations. This appears strange at first glance, but it can be rationalized in terms of a strong noncollinear ferromagnetic coupling between the two nearest neighboring Dy^{3+} cations within one circle (and consequently, they show a giant moment of 17.28 μ_B as a whole), according to the configuration of the Dy^{3+} cations in the molecule, Figure S1 (Supporting Information). It is noteworthy that when the moment $\mu_0 = 10\ \mu_B$ for one Dy^{3+} cation and $\mu_0 = 30\ \mu_B$ for three Dy^{3+} cations are employed, as also displayed in Figure 3, the experimental results cannot be fitted.

Because of the paramagnetic property of compound **6**, the Curie−Weiss Law, $\chi = C/(T - \Theta)$, was used for fitting the experimental $\chi - T$ curve of this complex. As can be found in Figure 4, the theoretical fitting curve is in excellent agreement with the experimental result for $C = 72.38$ emu K mol^{-1} and $\Theta = -4.46$ K, among which the value of C is slightly larger than the fitting result of $M - H$ at 2 K ($C = N\mu_0^2/3k = 51.02$ emu K mol^{-1}). Nevertheless, the very small value of Θ, −4.46 K, clearly reveals a very weak antiferromagnetic coupling between the neighboring Dy^{3+} cation circles despite the strong near-ferromagnetic coupling between the two Dy^{3+} cations within the circle.[2d]

Similar paramagnetic properties were also revealed for compounds **2**, **4**, **5**, **7**, **8**, and **9**. Figures S2, S4, S6, S8, S10, and S12 (Supporting Information) show the experimental $M - H$ curves and the theoretical fitting of **2**, **4**, **5**, **7**, **8**, and **9**. The fitting parameters of μ_0 (μ_B) and N obtained by the Langevin function are 3.03 and 1.14×10^{24} for **2**, 13.26 and 9.62×10^{23} for **4**, 16.04 and 7.64×10^{23} for **5**, 18.24 and 7.69×10^{23} for **7**, 11.89 and 7.35×10^{23} for **8**, and 7.27 and 1.65×10^{24} for **9**, respectively.

Figures S3, S5, S7, S9, S11, and S13 (Supporting Information) display the experimental $\chi - T$ curves and the theoretical fitting by the Curie−Weiss Law for compounds **2**, **4**, **5**, **7**, **8**, and **9**. Accordingly, the fitting parameters of C (emu K mol^{-1}) and Θ (K) are 7.69 and −3.97 for **2**, 36.94 and −1.35 for **4**, 23.85 and −2.11 for **5**, 44.07 and −3.88 for **7**, 10.70 and −3.23 for **8**, and 36.72 and −3.88 for **9**, respectively.

Conclusion

In summary, a series of 10 novel polyoxometalate(W/Mo) compounds connected via trivalent lanthanide cations as bridge have been prepared with the abduction of Al^{3+}. X-ray diffraction analyses reveal the three-dimensional framework of these complexes. Magnetic measurements reveal the paramagnetic properties and a strong ferromagnetic coupling between the two nearest neighboring lanthanide cations, Ln^{3+} (Ln = Dy, Er), within the circle for compounds **2** and **4**−**9**. Investigations of the optical, electronic, and catalytic properties of these newly synthesized compounds are in progress.

Experimental Section

Synthesis of Compounds 1−10. $Na_2WO_4 \cdot 2H_2O$ (2.35 g, 7 mmol), $(NH_4)_6Mo_7O_{24} \cdot 4H_2O$ (1.23 g, 1 mmol), and $Al_2(SO_4)_3 \cdot 18H_2O$ (0.19 g, 0.3 mmol) were dissolved in 45 mL of pure water. The suspension was stirred as it become clear via the slow addition of 10% hydrochloric acid, followed by the dropwise addition of 3 mL of an aqueous solution of Ln^{3+} (0.2 M), which was prepared by dissolving 0.3 mmol of Ln_2O_3 in nitrate acid and adjusting the pH of the resulting mixture to 4.44 using a 0.5 M potassium acetate solution. After filtration of the resulting solution, the filtrate was evaporated slowly at room temperature, and small colorless block crystals were isolated a few days later.

Compound 1. Yield: 0.04 g (4%). Anal. Calcd for $H_{88}K_4La_4W_{21.56}Mo_{2.44}O_{124}$: K, 2.24; La, 7.96; W, 56.77; Mo, 3.35. Found: K, 2.22; La, 7.94; W, 56.75; Mo, 3.38. IR data (KBr, cm^{-1}): 3420, 1637, 1400, 950, 900, 836, 633, 484.

Compound 2. Yield: 0.03 g (3%). Anal. Calcd for $H_{96}K_4Sm_4W_{22.04}Mo_{1.96}O_{128}$: K, 2.19; Sm, 8.42; W, 56.73; Mo, 2.63. Found: K, 2.22; Sm, 8.41; W, 56.75; Mo, 2.64. IR data (KBr, cm^{-1}): 3429, 1633, 1402, 952, 903, 840, 642, 479.

Compound 3. Yield: 0.04 g (4%). Anal. Calcd for $H_{96}K_4Eu_4W_{21.32}Mo_{2.68}O_{128}$: K, 2.21; Eu, 8.58; W, 55.32; Mo, 3.63. Found: K, 2.20; Eu, 8.57; W, 55.31; Mo, 3.65. IR data (KBr, cm^{-1}): 3411, 1630, 1409, 956, 909, 841, 646, 480.

Compound 4. Yield: 0.02 g (2%). Anal. Calcd for $H_{96}K_4Gd_4W_{21.56}Mo_{2.44}O_{128}$: K, 2.19; Gd, 8.82; W, 55.61; Mo, 3.28. Found: K, 2.20; Gd, 8.83; W, 55.60; Mo, 3.30. IR data (KBr, cm^{-1}): 3413, 1635, 1400, 954, 906, 839, 644, 485.

Compound 5. Yield: 0.02 g (2%). Anal. Calcd for $H_{96}K_4$-$Tb_4W_{20.88}Mo_{3.12}O_{128}$: K, 2.21; Tb, 8.99; W, 54.26; Mo, 4.23. Found: K, 2.23; Tb, 8.96; W, 54.26; Mo, 4.27. IR data (KBr, cm^{-1}): 3407, 1635, 1400, 954, 906, 840, 645, 485.

Compound 6. Yield: 0.75 g (70%). Anal. Calcd for $H_{96}K_4$-$Dy_4W_{20.96}Mo_{3.04}O_{128}$: K, 2.20; Dy, 9.16; W, 54.30; Mo, 4.11. Found: K, 2.22; Dy, 9.16; W, 54.32; Mo, 4.13. IR data (KBr, cm^{-1}): 3431, 1630, 1438, 955, 902, 847, 632, 486.

Compound 7. Yield: 0.03 g (3%). Anal. Calcd for $H_{84}K_4$-$Ho_4W_{20.84}Mo_{3.16}O_{122}$: K, 2.24; Ho, 9.44; W, 54.83; Mo, 4.33. Found: K, 2.26; Ho, 9.45; W, 54.84; Mo, 4.32. IR data (KBr, cm^{-1}): 3446, 1636, 1400, 951, 903, 839, 632, 487.

Compound 8. Yield: 0.42 g (39%). Anal. Calcd for $H_{96}K_4$-$Er_4W_{21.16}Mo_{2.84}O_{128}$: K, 2.19; Er, 9.32; W, 54.54; Mo, 3.82. Found: K, 2.20; Er, 9.31; W, 54.55; Mo, 3.82. IR data (KBr, cm^{-1}): 3417, 1637, 1401, 952, 900, 836, 633, 485.

Compound 9. Yield: 0.63 g (60%). Anal. Calcd for $H_{84}K_4$-$Yb_4W_{22}Mo_2O_{122}$: K, 2.20; Yb, 9.72; W, 56.79; Mo, 2.69. Found: K, 2.24; Yb, 9.72; W, 56.81; Mo, 2.72. IR data (KBr, cm^{-1}): 3428, 1640, 1402, 950, 901, 840, 634, 487.

Compound 10. Yield: 0.02 g (2%). Anal. Calcd for $H_{96}K_4$-$Lu_4W_{21.76}Mo_{2.24}O_{128}$: K, 2.18; Lu, 9.70; W, 55.44; Mo, 2.98. Found: K, 2.20; Lu, 9.68; W, 55.44; Mo, 2.93. IR data (KBr, cm^{-1}): 3436, 1639, 1401, 952, 900, 837, 635, 481.

X-ray Crystallography. Intensity data collection was carried out on a Siemens SMART diffractometer equipped with a CCD detector using Mo Kα monochromatized radiation ($\lambda = 0.71073$ Å) at 293(2) K. The absorption correction was based on multiple and symmetry-equivalent reflections in the data set using the SADABS program, based on the method of Blessing. The structures were solved by direct methods and refined by full-matrix least-squares using the SHELX-TL package.[26] Crystallographic data for compounds **1**−**10** are given in Table 1. Selected bond lengths and bond angles are listed in Table S2−S11 in the Supporting Information. The essential atomic coordinates and equivalent isotropic displacement parameters are listed in Table S12−S21 also in the Supporting Information.

Magnetic Measurements. The magnetic susceptibility and magnetization of a powdered sample were recorded on a Quantum Design SQUID magnetometer on the MPMS-7 system.

Acknowledgment. Financial support from NSFC (Grant 20325105, 20431010), the National Ministry of Science and Technology of China (Grant 2001CB6105-07), and the Ministry of Education of China is acknowledged.

Supporting Information Available: The circle used in the fitting of $M-H$ for compounds **6** and **8**, the dependence of magnetization on the external magnetic field for compounds **2** and **4**−**9** at 2 K, the magnetic behavior of compounds **2** and **4**−**9** measured at an external magnetic field of 10 000 Oe, the fitting parameters of μ_0, N, C, and Θ for complexes **2**, **4**, and **5**−**9**, selected bond lengths (Å) and angles (deg) for complexes **1**−**10**, and atomic coordinates ($\times 10^4$) and equivalent isotropic displacement parameters ($\times 10^3$ Å^2) for complexes **1**−**10**. This material is available free of charge via the Internet at http://pubs.acs.org. Crystallographic data (excluding structure factors) for these structures have been deposited with the Inorganic Crystal Structure Database as Supplementary Publications 416568 for **1**, 416570 for **2**, 416565 for **3**, 416566 for **4**, 416571 for **5**, 416563 for **6**, 416567 for **7**, 416564 for **8**, 416572 for **9**, and 416569 for **10**. Copies of the data can be obtained free of charge on application to ICSD, Fachinformationzentrum Karlsruhe, 76344 Eggenstein-Leopoldhafen, Germany (fax +49-(0)7247-808-666; e-mail crysdata@fiz-karlsruhe.de).

IC0612597

---

(26) Sheldrick, G. M. *SHELXTL-97: Program for Refinement of Crystal Structures*; University of Göttingen: Göttingen, Germany, 1997.